# Generation of Chimeric Antigen Receptor Macrophages from Human Pluripotent Stem Cells to Target Glioblastoma

Gyuhyung Jin[a,b], Yun Chang[a,b], Xiaoping Bao[a,b,*]

[a] Davidson School of Chemical Engineering, Purdue University, West Lafayette, IN 47907, USA

[b] Purdue University Center for Cancer Research, West Lafayette, IN 47907, USA

[*] Corresponding author: bao61@purdue.edu

## Abstract

Glioblastoma (GBM) is an aggressive brain tumor giving a poor prognosis with the current treatment options. The advent of chimeric antigen receptor (CAR) T cell therapy revolutionized the field of immunotherapy and has provided a new set of therapeutic options for refractory blood cancers. As an effort to apply this therapeutic approach to solid tumors, various immune cell types and CAR constructs are being studied. Notably, macrophages have recently emerged as potential candidates for targeting solid tumors, attributed to their inherent tumor-infiltrating capacity and abundant presence in the tumor microenvironment. In this study, we developed a chemically defined differentiation protocol to generate macrophages from human pluripotent stem cells (hPSCs). A GBM-specific CAR was genetically incorporated into hPSCs and the CAR hPSC-derived macrophages exhibited potent anti-cancer activity against GBM cells *in vitro*. Our findings demonstrate the feasibility of generating functional CAR-macrophages from hPSCs for adoptive immunotherapy, thereby opening new avenues for the treatment of solid tumors, particularly GBM.

**Keywords**: hPSC-derived macrophages, CAR-macrophages, adoptive immunotherapy for Glioblastoma

## 1. Introduction

Immunotherapy has emerged as a promising approach to combating cancer over the last few decades. Advances in immune checkpoint inhibitors and chimeric antigen receptor (CAR) T cell therapy have introduced attractive therapeutic options for treating cancers with their potential in targeting refractory cancers and many successful clinical cases [1]. Particularly, CAR T cell therapy, which utilizes modified cytotoxic T cells to target a specific cancer antigen, has showed promising results in treating refractory blood cancers, leading to the approval of six CAR T cell therapies by the United States Food and Drug Administration (FDA) as of 2022 [2]. However, challenges such as low efficacy in treating solid tumors, lengthy process, and high cost remain in current CAR T therapy. To address these issues, instead of using autologous T cells, the use of off-the shelf immune cell products derived from human pluripotent stem cells (hPSCs) has been suggested as an alternative approach [3]. Not only hPSC-derived T cells [4], but also other immune cells such as hPSC-natural killer (NK) cells [5] and hPSC-macrophages [6] engineered with CARs have been tested for their anti-tumor activity at the pre-clinical and clinical levels [7]. In addition to these immune cell types, our lab generated CAR-neutrophils from hPSCs for targeted cancer immunotherapy [8], where chlorotoxin (CLTX), a 36-amino acid peptide that specifically targets glioblastoma (GBM) [9], was incorporated into a CAR structure and the CLTX CAR-neutrophils showed superior anti-tumor activity compared to the unmodified hPSC-derived neutrophils. As neutrophils and macrophages are the major innate immune cells that share many important functional and molecular characteristics, we hypothesized that CAR-macrophages would also be effective in targeting GBM. Furthermore, macrophages associated with the tumor constitute up to 50% of the cellular composition in GBM. Among these macrophages, approximately 85% are infiltrating macrophages/monocytes, while the remaining 15% are brain-resident macrophages, also known as microglia [10]. This significant presence and distribution of macrophages in the GBM microenvironment underscore the potential importance of these cells in the context of GBM pathobiology. Macrophages are gaining attention as new effector cells for immunotherapy not only because of their innate phagocytic activity and regulatory function but also their capability to infiltrate into tissues and abundance in the tumor microenvironment [11–15]. Based on our earlier hematopoietic progenitor and stem cell differentiation platform [16], we developed a feeder-free macrophage differentiation protocol utilizes macrophage colony-stimulating factor (M-CSF) as the single differentiation factor after hematopoietic progenitor stage. Our hPSC-derived macrophages (hPSC-M) showed general molecular characteristics of primary macrophages and

exhibited phagocytic activity. Notably, CLTX CAR hPSC-M displayed improved cytotoxicity against U87MG GBM cells compared to the unmodified hPSC-M. Our results demonstrate that functional CAR-macrophages targeting GBM could be produced from hPSCs for adoptive immunotherapy against cancers.

## 2. Material and methods

### hPSC maintenance and macrophage differentiation

H9 hESC line (WiCell) and CLTX CAR H9 line [8] were maintained on Matrigel (Corning, 354230)-coated tissue culture-treated (TC) plates in mTeSR™ Plus medium (STEMCELL Technologies, 100-0276) at 37℃, 5% CO2. The medium was changed daily. When the cells reached 70-80% confluency, they were dissociated with 0.5 mM EDTA (Invitrogen, 15575-038) and plated on a new Matrigel-coated TC plate with a split ratio of 1:10 in mTeSR™ Plus medium containing 5 μM ROCK inhibitor Y-27632 (Cayman Chem, 10005583). Matrigel-coated plates were prepared by adding 0.08 mg/mL Matrigel in DMEM/F12 medium (Gibco, 11330-032) to TC plates and incubating at 37 °C for at least 2 hours. For macrophage differentiation, cells were dissociated with 0.5 mM EDTA and plated either on a diluted Matrigel (0.004 mg/mL)-coated 24-well TC plates in mTeSR™ Plus medium with 5 μM Y-27632 or on 24-well TC plates in mTeSR™ Plus medium containing 0.5 μg/mL iMatrix-511 (Iwai North America, 892012) and 5 μM Y-27632 (day -1). 400 μL of medium was used for each well of 24-well plates. At day 0, the medium was changed with DMEM (Gibco, 11965118) supplemented with 100 mg/mL ascorbic acid (Sigma, A8960) (DMEM/Vc) containing 6 μM CHIR99021 (Cayman Chem, 13122). At day 1, the medium was changed with advanced DMEM/F12 supplemented with 2.5 mM GlutaMAX (Gibco, 35050–061) and 100 mg/mL ascorbic acid (LaSR basal). At day 2 and day 3, the medium was changed with LaSR basal containing 50 ng/ml VEGF (PeproTech, 100-20). At day 4, the medium was changed with Stemline II medium (Sigma, S0192) containing 50 ng/ml of SCF (PeproTech, 300-07), 50 ng/ml FLT3L (PeproTech, 300-19), and 10 μM SB-431542 (Cayman Chem, 13031). At day 6, the medium was changed with Stemline II medium containing 50 ng/ml of SCF, 50 ng/ml FLT3L, 50 ng/ml thrombopoietin (TPO) (PeproTech, 300-18), 10 ng/ml Interleukin 3 (IL-3) (PeproTech, 200-03), 50 ng/ml Interleukin 6 (IL-6) (PeproTech, 200-06), and 5% (v/v) human serum albumin (HSA) (Valley Biomedical, HP1022HI). At day 9, half of the medium was removed and replaced with 400 μL fresh Stemline II medium containing 10 ng/ml IL-3, 50 ng/ml IL-6, 50 ng/ml M-CSF (PeproTech, 300-25), and 5% (v/v) HSA. At day 12, floating

cells were gently harvested, filtered through a 100 μm strainer (Fisher Scientific, 22363549) sitting on a 50 mL tube, spun down, and resuspended in Stemline II medium containing 50 ng/ml M-CSF. 400 μL of fresh Stemline II medium containing 50 ng/ml M-CSF was added to each well of 24-well plate every 4 days until day 32.

**U87MG and MDA-MB-231 maintenance**

U87MG GBM cells that express luciferase were maintained on tissue-culture treated plates in MEM medium (Gibco, 32561037) containing 10% fetal bovine serum (FBS) (v/v) (Gibco, 26140) at 37℃, 5% $CO_2$. MDA-MB-231 cells that express luciferase were maintained on tissue-culture treated plates in DMEM/F12 medium containing 10% FBS (v/v). The medium was changed every three days. When the cells reached confluency, they were passaged using 0.25% Trypsin-EDTA (Gibco, 25200072).

**Engineering of CLTX CAR hPSCs**

The CLTX CAR H9 cell line was generated as previously described [8]. Briefly, AAVS1 CLTX CAR donor plasmid was constructed by cloning a directly synthesized CLTX CAR sequences (GeneWiz) into AAVS1-Puro CAG-FUCCI donor plasmid (Addgene; #136934). H9 cells were treated with 10 μM Y-27632 overnight, followed by incubation in Accutase (ICT, AT104-500) for 10 minutes. Subsequently, the cells were nucleofected with 6 μg of SpCas9 AAVS1 gRNA T2 (Addgene; #79888) and 6 μg of the CAR donor plasmids. The nucleofected cells were then seeded onto a Matrigel-coated 6-well plate and incubated in mTeSR™ Plus medium containing 10 μM Y-27632 overnight, with a daily medium change afterwards. Upon reaching 80-90% confluence, cells were subjected to drug selection under 1 μg/mL puromycin (Gibco, A11138-03). After cell recovery, individual colonies were selected and expanded for further experimental analysis.

**Genomic DNA extraction and genotyping of CLTX CAR H9**

The genomic DNA extraction and genotyping were performed according to the previous method [8]. Briefly, genomic DNA from each clone of CLTX CAR H9 was extracted using QuickExtract™ DNA Extraction Solution (Epicentre, QE09050). GoTaq Green Master Mix (Promega, 7123) was used to screen extracted genomic DNA. The primers used as follows;
CLTX CAR genotyping:
FWD: CTGTTTCCCCTTCCCAGGCAGGTCC

RVS: TCGTCGCGGGTGGCGAGGCGCACCG

Homozygosity genotyping:

FWD: CGGTTAATGTGGCTCTGGTT

RVS: GAGAGAGATGGCTCCAGGAA

**Immunofluorescence**

Cells were washed with PBS and fixed in 4% paraformaldehyde (PFA) diluted in PBS for 15 min at room temperature. The fixed cells were washed with PBS three times and incubated in diluted antibodies in PBS containing 5% nonfat dry milk (w/v) (Bio-Rad, 1706404) and 0.4 % Triton X-100 (v/v) (Fisher Scientific, BP151-500) overnight at 4 °C. On the next day, the cells were washed with PBS three times. In the case of unconjugated antibodies, the cells were incubated in diluted secondary antibodies in PBS containing 5% nonfat dry milk and 0.4 % Triton X-100 for 30 min at room temperature, washed with PBS three times, and incubated in PBS containing 10 μg/ml Hoechst 33342 (Invitrogen, H3570) for 5 min at room temperature. In the case of the conjugated antibodies, cells were incubated in Hoechst 33342 without secondary antibody staining. After nuclei staining, cells were washed with PBS two times and imaged under a fluorescence microscope (Leica, DMi-8). Antibodies used for immunofluorescence and corresponding dilution ratio were listed as follows; anti-NANOG (Cell Signaling Technology, 3580S/1:800), anti-OCT (Cell Signaling Technology, 2750S/1:200), anti-CD34-APC (Miltenyi Biotec, 130-113-176/1:50), anti-CD34-FITC (Miltenyi Biotec, 130-113-178/1:50), anti-RUNX1-Alexa Fluor® 488 (Abcam, ab199221/1:100), anti-SOX17-APC (R&D Systems, IC1924A/1:100), anti-Rabbit IgG Alexa Fluor® 488 (Invitrogen, A21441/1:1000), Actin stain ™ 488 Phalloidin (Cytoskeleton, PHDG1/1:50), anti-CD45-APC (BD Biosciences, 560973/1:50).

**Flow cytometry analysis**

hPSCs were harvested by incubating in Accutase for 8 minutes at 37°C, 5% $CO_2$. Subsequently, cells were centrifuged at 200 xg for 5 minutes and then fixed in 1% paraformaldehyde (PFA) diluted in PBS for 20 minutes at room temperature, followed by another centrifugation step. The supernatant was carefully removed, and the pelleted cells were washed three times with 2 ml of PBS containing 2.5% bovine serum albumin (BSA). Next, cells were incubated overnight at 4°C in 100 μl of diluted antibodies in PBS containing 2.5% BSA and 0.1% Triton X-100. On the following day, the cells were washed twice with PBS containing 2.5% BSA and 0.1%

Triton X-100, resuspended in PBS containing 2.5% BSA, and subjected to analysis using a flow cytometer (Accuri C6 plus, Beckton Dickinson).

Floating hematopoietic cells were collected and filtered through a 100 μm strainer. After centrifugation (200 xg, 5 min), cells were washed with PBS containing 2.5% bovine serum albumin (BSA) (w/v) (Sigma, A9418), spun down, and incubated in 50 μl diluted antibodies in PBS containing 2.5% BSA for 30 min at room temperature in the dark. Cells were then further diluted in 300 μl PBS containing 2.5% bovine serum albumin and analyzed using a flow cytometer. Antibodies used for flow cytometry and corresponding dilution ratio were listed as follows:

anti-NANOG (Cell Signaling Technology, 3580S/1:500), anti-OCT (Cell Signaling Technology, 2750S/1:500), anti-Human IgG4 pFc'-FITC (Southern BioTech, 9190-02/1:50), anti-CD43-APC (BD Biosciences, 560198/1:50), anti-CD45-PE (BD Biosciences, 555483/1:50), anti-CD14-Alexa Fluor® 488 (BD Biosciences, 561706/1:50), anti-CD14-APC (BD Biosciences, 561708/1:50), anti-CD11b-APC (BD Biosciences, 561015/1:50), anti-CD44-FITC (BD Biosciences, 555478/1:50), anti-CD235a-FITC (BD Biosciences, 559943/1:50), anti-CD45-APC (BD Biosciences, 560973/1:50), anti-CD68-Alexa Fluor® 647 (BD Biosciences, 562111/1:50), anti-CD172a-Alexa Fluor® 647 (BD Biosciences, 565035/1:50), anti-CD86-APC (BD Biosciences, 374208/1:50), anti-CD163-APC (BD Biosciences, 326510/1:50).

**Reverse transcription polymerase chain reaction (RT-PCR) assay**

RNA from hPSC-derived macrophages and H9 hPSCs were extracted using Direct-zol™ RNA MiniPrep Plus (Zymo Research, R2072). cDNA was synthesized from the extracted RNA using ZymoScript™ RT PreMix Kit (Zymo Research, R3012). GoTaq Green Master Mix was used to screen macrophage markers. The primers used as follows:

CD14: CCGCTGTGTAGGAAAGAAGC (FWD); GCAGCGGAAATCTTCATCGT (RVS)
CD16: AAATGCTTTCTTGGCCAGGG (FWD); TTGTCTTCTCCATCCCCACC (RVS)
CD11b: ATCTCAACTTCACGGCCTCA (FWD); ACGGGATGTCACACTGGATT (RVS)
CD64: CTCAGGCATGGGAAAGCATC (FWD); TTGCTGCCCATGTAGAAGGA (RVS)
CD68: GGAGACTACACGTGGACCAA (FWD); CATTGTACTCCACCGCCATG (RVS)
CCR5: TTTGCGTCTCTCCCAGGAAT (FWD); CCCTGTGCCTCTTCTTCTCA (RVS)
MSR1: AGGACACTGATAGCTGCTCC (FWD); ACTGCAAACACGAGGAGGTA (RVS)

**Wright-Giemsa staining**

hPSC-derived macrophages were fixed on a glass slide using methanol and stained with Wright-Giemsa solution (Sigma, WG16) according to the manufacturer's protocol.

**Phagocytosis assay**

The phagocytic activity of hPSC-derived macrophages was assessed using pHrodo™ Green *E.coli* BioParticles™ Conjugate (Invitrogen, P35366). The *E.coli* beads were diluted in culture medium (1:100 dilution), sonicated with an ultra-sonicator three times, and added to the cells. After 12 hours, cells were imaged under the fluorescence microscope. Then cells were stained with anti-CD14-APC antibody and analyzed using a flow cytometer. % cells phagocytosed particles was obtained after gating $CD14^+$ population.

**Cytokine secretion assay**

hPSC-derived macrophages were collected, centrifuged, and resuspended in Stemline II medium containing 50 ng/ml M-CSF, with or without 5x lipopolysaccharide (LPS) (Invitrogen, 00-4976-93). Subsequently, cells were seeded on a 96-well plate. After 24 hours, the supernatant was collected and subjected to analysis using a human TNF-alpha ELISA kit (Invitrogen, BMS223-4) and a human IL-6 ELISA kit (Invitrogen, BMS213-2), following the manufacturer's instructions.

**M1 polarization test**

hPSC-derived macrophages were harvested, centrifuged, and suspended in Stemline II medium supplemented with 50 ng/ml M-CSF, with or without 5x lipopolysaccharide (LPS). After incubation for 24 hours, cells were collected and subjected to flow cytometry analysis to evaluate the expression of CD86 (M1 marker) and CD163 (M2 marker).

**Primary monocyte isolation and macrophage differentiation**

Donor blood cells were subjected to centrifugation (300 xg, 5 minutes) and subsequently washed with PBS containing 1% FBS. Cells were then incubated in 1x red blood cell lysis buffer (BD Pharm Lyse™, BD Biosciences, 555899) for 15 minutes at room temperature in dark. Following lysis, cells were centrifuged and washed with PBS containing 1% FBS for three times. The resulting cells were stained with anti-CD14-FITC (BD Biosciences, 561712) at a 1:50 dilution in PBS containing 2.5% BSA for 30 minutes in dark. Subsequently, CD14+

cells were isolated using magnetic-activated cell sorting (MACS) with EasySep™ Magnet (STEMCELL Technologies, 18000) according to the manufacturer's instructions. Isolated CD14+ cells were cultured in RPMI 1640 medium supplemented with 10% FBS, 2.5mM GlutaMAX, and 50 ng/ml M-CSF for 7 days, with fresh medium changed every three days.

**Cytotoxicity assay**

U87MG GBM and MDA-MB-231 cells that express luciferase were collected and plated in a 96-well plate (10,000 cells in 100 μL of MEM or DMEM + 10% FBS medium per well). hPSC-derived macrophages were added to the same well with an appropriate effector-to-target ratio in 100 μL of MEM or DMEM + 10% FBS per well). The mixture was incubated for 24 hours or 48 hours. After incubation, the cells were washed with PBS two times to remove floating macrophages and incubated in MEM or DMEM medium containing 150 μg/ml D-luciferin (Cayman Chem, 14681) for 30 min at 37°C, 5% $CO_2$. After incubation, bioluminescence was measured using a plate reader (Molecular Devices, SpectraMax® iD3). The % of tumor cell killing was calculated by dividing the luminous intensity of the co-incubated well with the luminous intensity of the control (tumor cell only) well after background subtraction.

## 3. Results and Discussion

### Generation of CLTX CAR hPSCs

The CLTX CAR structure constructed in our previous study is composed of a signaling peptide, a GBM-targeting CLTX peptide as an antigen-binding domain, IgG4 spacer, CD4 transmembrane domain, and CD3ζ signaling domain [8] (**Figure 1A**). While this first-generation CAR construct was originally designed for T cells and lacks co-stimulatory domains, it was still effective in mediating an anti-cancer cell activity of hPSC-derived neutrophils both *in vitro* and *in vivo*. Zhang *et al*. demonstrated that the macrophage-specific CAR construct composed of CD86 and FcγRI signaling domain along with CD8α transmembrane was effective in mediating *in vitro* and *in vivo* cytotoxicity of hPSC-derived macrophages against tumor cells [6]. On the other hand, CD3ζ-based CARs also directed anti-cancer activity of human macrophage THP-1 cell line [15]. Based on these studies and the similarity between neutrophils and macrophages in terms of their physiological functions, we hypothesized that the CD3ζ-based CLTX CAR construct would also work effectively in macrophages. CRISPR/Cas9 genome editing was used to generate CLTX CAR H9 hPSCs via homology directed repair (HDR) followed by puromycin (Puro) selection, and single cell-derived hPSC clones were genotyped

to validate the successful insertion of CLTX CAR construct (**Figure 1B**). Among the eight clones analyzed, five clones were heterozygous, and one clone was homozygous. The homozygous clone was picked for further experiments. Both unmodified hPSCs and CLTX CAR hPSCs maintained high expression levels of pluripotency markers (**Figure 1C**) and CLTX CAR hPSCs retained the expression of CAR construct (**Figure 1D**).

**Molecular characterization of hematopoietic progenitor and macrophage-like cells during macrophage differentiation from hPSCs**

Previously, our lab developed a feeder-free culture platform for the generation of hemogenic endothelium and the subsequent generation of definitive hematopoietic progenitor cells from hPSCs [16]. Starting day 4 of the differentiation, clusters of hemogenic endothelial cells that express CD34, SOX17, and RUNX1 appeared on the culture plate (**Figure 2A-B**) [16]. At around day 9 of the differentiation, hematopoietic progenitor cells started to bud out from the hemogenic endothelium. These cells were either loosely sitting on the endothelium or floating around in the culture wells and expressed definitive hematopoietic marker, RUNX1, and pan-hematopoietic marker, CD45 (**Figure 2C**). To induce myeloid and macrophage lineage commitment, the protocol was slightly modified to include myeloid-priming cytokines such as IL-3, IL-6, TPO, and M-CSF after the formation of hemogenic endothelium (**Figure 2A**). IL-3 and IL-6 are cytokines that are typically used to induce myeloid differentiation and were shown to induce myeloid specification and subsequent neutrophil differentiation from hPSCs [8]. TPO is a cytokine that typically induces the formation of megakaryocytes but was also used to generate myeloid progenitors from hPSCs, along with M-CSF, a macrophage-lineage-specific growth factor [17]. Filtering day 12 floating hematopoietic cells through a 100 μm strainer resulted in a relatively pure population (>90%) of CD43 and CD45 double-positive cells that did not express primitive marker CD235a (**Figure 2D**). The presence of RUNX1 and CD44 further confirmed their definitive hematopoietic progenitor (**Figure 2B-D**). Previous studies generated macrophages from hPSCs with a typical M-CSF treatment at the later stages of differentiation in the presence of other cytokines [6,17–20], and some protocols employed M-CSF only after the collection of floating hematopoietic progenitors [18,19]. To evaluate whether M-CSF alone is sufficient to induce macrophage differentiation from our hPSC-derived myeloid progenitors, day 12 cells were subjected to further differentiation with or without M-CSF and subjected for flow cytometry analysis of CD14 and CD11b expression at day 32. As expected, the addition of 50 ng/ml M-CSF significantly increased the proportion of $CD14^+$ and

$CD11b^+$ cells as compared to conditions without M-CSF or with 10 ng/ml M-CSF (**Figure 2E**). Notably, the addition of M-CSF alone consistently yielded a highly pure population of $CD14^+$ and $CD11b^+$ macrophage-like cells across multiple differentiation batches (**Figure 2F**).

**Characterization of hPSC-derived macrophage-like cells (hPSC-M)**

To produce hPSC-derived macrophage-like cells, we used M-CSF as the single differentiation factor after collecting floating cells at day 12 for further experiments (**Figure 3A**). Both unmodified hPSC-derived (hPSC-M) and CLTX CAR hPSC-derived macrophage-like cells (CLTX hPSC-M) displayed high expression levels of CD14 and CD11b (>80%), two surface markers of macrophages and myeloid cells (**Figure 3B**). The resulting $CD14^+$ cells also expressed CD68 and CD172a (SIRPα), two additional markers associated with macrophages (**Figure 3C**). RT-PCR analysis showed that various pan-macrophage markers are expressed in hPSC-M (**Figure 3D**). Consistent with previous reports, hPSC-M exhibited typical morphology of monocytes/macrophages (**Figure 3E**) [18,21]. Notably, cytoplasmic vacuoles were observed in hPSC-M, one of the morphological characteristics that are seen in macrophages undergoing pinocytosis [22]. Lipopolysaccharide (LPS) is well-known to induce the secretion of cytokines such as IL-6 and TNF-α from macrophages [23]. To assess their ability to release cytokines in response to LPS, both unmodified and CLTX hPSC-M were cultured in LPS-containing media for 24 hours, and the secretion of IL-6 and TNF-α was quantified via ELISA. A significant increase in the secretion of both IL-6 and TNF-α was observed in LPS-treated hPSC-M, and CLTX hPSC-M exhibited even higher levels of IL-6 and TNF-α secretion as compared to hPSC-M (**Figure 3F**). Another hallmark of macrophages is their ability to polarize into either M1 (classically activated, pro-inflammatory) or M2 (alternatively activated, anti-inflammatory) subtype[24]. To determine their M1 polarization, unmodified and CLTX hPSC-M were treated with LPS for 24 hours, and the expression levels of CD86 (M1 marker) and CD163 (M2 marker) were assessed using flow cytometry. Analysis based on the median fluorescence intensity (MFI) of these markers revealed a slight increase in CD86 expression in hPSC-M, while a significant phenotype change was not observed in CLTX hPSC-M (**Figure 3G**). Both hPSC-M and CLTX hPSC-M showed a significant decrease in the expression of CD163 after LPS treatment, suggesting a M1 polarization in these cells. Taken together, the addition of M-CSF after the hematopoietic/myeloid progenitor state was sufficient to induce our hematopoietic progenitor cells into macrophage-like cells showing typical molecular

characteristics of monocytes/macrophages.

**Functional characterization of CLTX CAR hPSC-M**

To assess their phagocytic activity, unmodified and CLTX hPSC-M were exposed to *E. coli* bioparticles for 12 hours. Live cell imaging revealed that a substantial proportion of the bioparticles were internalized within the first 3 hours after incubation (**Supplementary Figure 1**). Subsequent flow cytometry analysis demonstrated that a majority of both $CD14^+$ hPSC-M and CLTX hPSC-M exhibited phagocytosis of bacterial particles, indicative of an active phagocytic behavior (**Figure 4A**). A significant difference in phagocytic activity was not observed between unmodified hPSC-M and CLTX hPSC-M. CAR T cells were reported to form nonclassical immune synapses at the interface between target cells to activate their cytotoxic signaling [25]. These immune synapses are characterized by actin accumulation at the interface of effector cells [26]. Interestingly, the formation of immune synapses was observed between hPSC-derived CAR-neutrophils and target tumor cells [8]. Like hPSC-derived CAR-neutrophils, CLTX hPSC-M incubated with U87MG GBM cells also showed an accumulation of F-actin at the interface between CLTX hPSC-M and tumor cells, which possibly indicates the formation of immune synapses mediated by CAR structure (**Figure 4B**). Lastly, hPSC-M and CLTX hPSC-M were incubated with luciferase-expressing U87MG cells for 24 hours to assess their cytotoxicity against the target cells. MDA-MB-231 breast cancer cell line was used as a negative control to validate the specificity of CAR-M. As expected, CLTX hPSC-M exhibited superior cytotoxicity against target cells as compared to the unmodified hPSC-M at an effector-to-target cell ratio of 3:1, 5:1, 10:1, and 20:1 (**Figure 4C**). Notably, CLTX hPSC-M displayed some levels of cytotoxicity against MDA-MB-231 cells, whereas unmodified hPSC-M promoted the growth of MDA-MB-231 cancer cells after a 24-hour coculture. Given a much lower cytokine secretion upon LPS treatment, these results may collectively suggest that hPSC-M was polarized towards the M2 pro-tumor subtype during differentiation, despite further investigation is needed. 48 hours after coculture, CLTX hPSC-M retained some degree of cytotoxicity against the target cells, while it is much less potent than that of 24-hour condition. The tumor cell killing activity of both hPSC-M and CLTX hPSC-M appeared to be reduced with time and variable 48 hours after coculture (**Supplementary Figure 2**), suggesting that the tumor-killing ability of hPSC-derived macrophage-like cells may be dependent on their initial phagocytic action. To compare the cytotoxicity of primary macrophages and hPSC-M, $CD14^+$ monocytes were isolated from human blood samples (**Supplementary Figure 3**) and

differentiated into macrophages in the presence of M-CSF. At an effector-to-target cell ratio of 10:1, CLTX hPSC-M exhibited a higher cytotoxicity against U87MG cells than that of primary macrophages (**Figure 4D**). These results demonstrated that the incorporation of CLTX CAR improved tumor killing ability of hPSC-derived macrophage-like cells [27].

## 4. Conclusion

Engineered CAR-macrophages have been shown to display an enhanced anti-cancer cell activity in recent studies [12–15]. As compared to macrophage cell lines or primary cells, hPSCs have been suggested as an unlimited cell source to produce off-the-shelf CAR-macrophages and a few studies have been conducted to generate CAR-macrophages from hPSCs [6,20]. Here, we reported the generation of CLTX CAR hPSC-M with a potent anti-cancer cell activity against U87MG GBM cells *in vitro*. Firstly, CRISPR/Cas9-mediated homologous recombination was employed to construct stable CAR hPSC. Among various successfully targeted clones, a single homozygous clone was meticulously chosen and employed throughout the entire study. It is worth noting that the utilization of a single clone may potentially constitute a limitation of this investigation, as distinct clones could conceivably exert unforeseen influences on the behavior of the cells. Subsequently, CLTX CAR hPSCs were differentiated into macrophages following our macrophage differentiation protocol. This protocol was established upon our previous feeder-free and monolayer-based hematopoietic progenitor differentiation platform, which involves the use of small molecule activation of Wnt signaling and subsequent formation of hemogenic endothelium by VEGF [8,16]. Different from other protocols, our approach does not utilize commonly used growth factors such as BMP4, Activin A, and FGF during the early stage of the differentiation process. In addition, M-CSF was used as the sole differentiation factor after the hematopoietic progenitor stage. As a result, our protocol yields a relatively pure population (>80%) of $CD14^+/CD11b^+$ macrophage-like cells that exhibit typical molecular characteristics of macrophages and respond to LPS stimulation. Previously, the utilization of a CAR construct comprising GBM-targeting CLTX peptide, CD4 transmembrane domain, and CD3ζ signaling domain was shown to enhance the cytotoxicity of hPSC-derived neutrophils against GBM cells[8]. This CAR construct exhibited superior cytotoxicity when compared to another CLTX CAR construct consists of NKD2G transmembrane domain, 2B4 co-stimulatory domain, and CD3ζ signaling domain, suggesting that the transmembrane and intracellular signaling mechanisms play important roles in

mediating neutrophils' immune activity. While this GBM-targeting CAR construct enhanced the tumor cell-killing capabilities of CAR hPSC-M compared to unmodified hPSC-M and primary macrophages, T cell-specific transmembrane and intracellular signaling domains were used and future studies should include macrophage-specific domains, including FcγRI [6], to further enhance anti-tumor activity of hPSC-M. Additionally, a CLTX CAR construct without CD3ζ signaling domain should be used as control in future studies to determine if the observed improvement of anti-tumor function in hPSC-M is simply due to the enhanced binding of hPSC-M to GBM cells. While hPSC-derived macrophages already showed their potential in targeting solid tumors in previous studies, targeting GBM with macrophages might provide a new approach to treat this aggressive cancer as glioma-associated microglia/macrophages are abundant in the tumor microenvironment [28]. This study suggests that either engineering the pro-tumor macrophages or replacing them with off-the-shelf macrophage products may alter the pro-tumorigenic microenvironment into anti-tumorigenic, thereby suppressing the tumor progression.

## Figures and figure captions

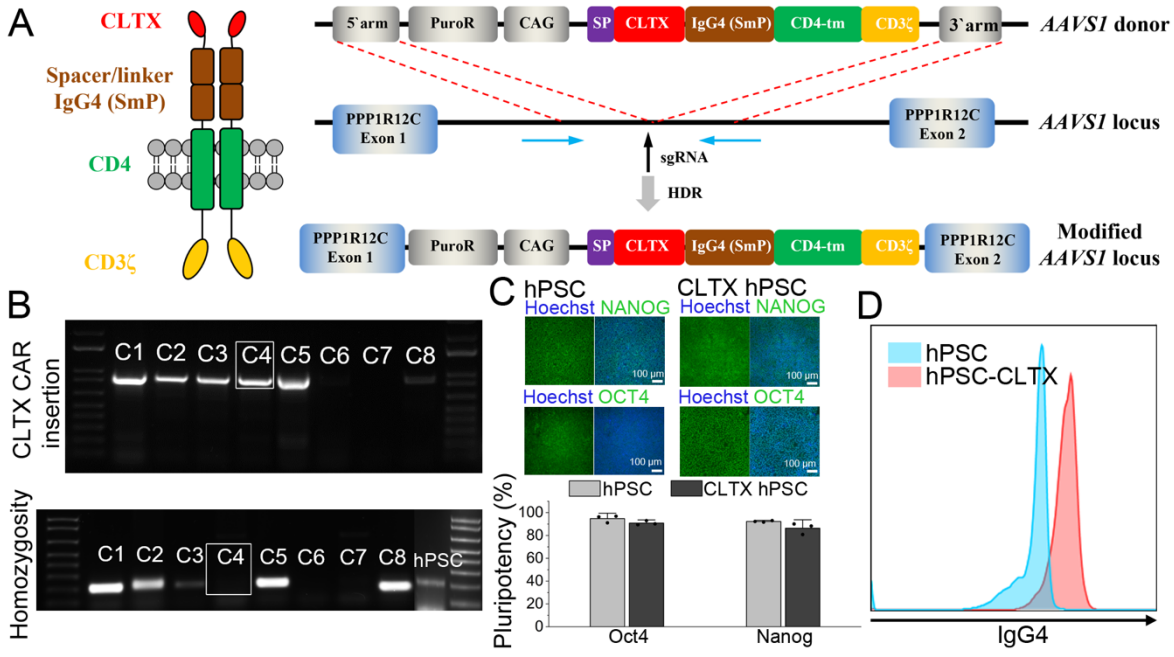


**Figure 1. Generation of CLTX CAR hPSCs.** (A) Schematic illustration showing the CLTX CAR construct and its insertion into *AAVS1* safe harbor locus (located between exon 1 and exon 2 of gene *PPP1R12C*) via CRISPR/Cas9 genome editing-mediated homology-directed repair (HDR). The CLTX

CAR construct consists of a signal peptide (SP), CLTX peptide, a Fc domain as a spacer (IgG4 (SmP)), CD4 transmembrane domain (CD4-tm), and CD3ζ cytoplasmic domain. Puromycin resistance gene (PuroR) is expressed by the constitute host gene expression at *AAVS1* site while the CLTX CAR construct is expressed by constitutive CAG promoter. Donor plasmid has both 3'and 5' homology arms which confer sequence homology for HDR. (B) Genotyping of CLTX CAR hPSC clones. The amplification for CLTX CAR insertion spans from the host genome to the inserted region. The presence of the band indicates the successful insertion into the *AAVS1* locus (expected amplicon size: 991 bp). The amplification for homozygosity spans the host genome only (expected amplicon size: 206 bp). With the correct insertion, no band is detected. (C) Immunofluorescence images and flow cytometry of H9 hPSC line (hPSC) and CLTX CAR H9 hPSC line (CLTX hPSC) for pluripotency marker expression. ($n$ = 3) (D) Expression of CAR construct in CLTX CAR hPSCs. Anti-IgG4 antibody was used to analyze the presence of IgG4 spacer in the CAR construct by flow cytometry. ($n$ = 4) Data represented as mean ± SD.

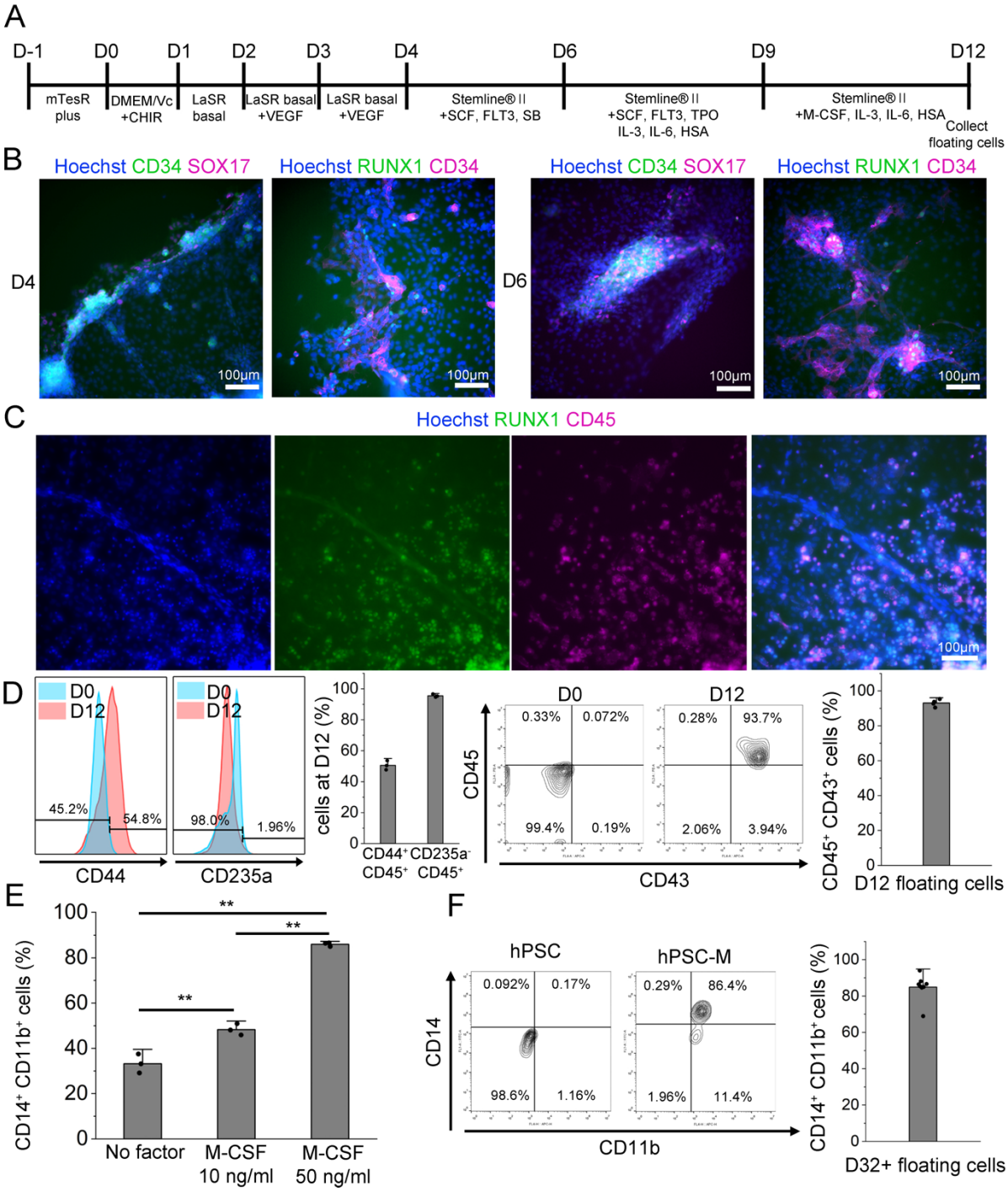


**Figure 2. Molecular characterization of hematopoietic progenitor and macrophage-like cells during macrophage differentiation from hPSCs.** (A) Schematic of timeline for macrophage differentiation before day 12. (B) Immunofluorescence images of cells at day 4 and day 6 of the hematopoietic/macrophage differentiation. Small clusters of cells started to express CD34, SOX17, and RUNX1. (C) Immunofluorescence image of cells at day 12 of the differentiation showing the round shaped RUNX1$^{+}$/CD45$^{+}$ floating progenitor cells. (D) Flow cytometry analysis of day 12 floating cells for CD44, CD235a, CD43 and CD45 expression. (*n*=3 independent differentiations) (E) Flow cytometry

analysis for CD14 and CD11b expression of day 32 floating cells on the conditions of no differentiation factor, 10 ng/ml M-CSF, and 50 ng/ml M-CSF after day 12. The statistical analysis was performed using a one-way ANOVA with Tukey's host hoc test (* $p < 0.05$ ** $p < 0.01$). (F) Flow cytometry analysis of day 32+ floating cells for CD14 and CD11b expression. n=9 independent differentiations. Data represented as mean ± SD.

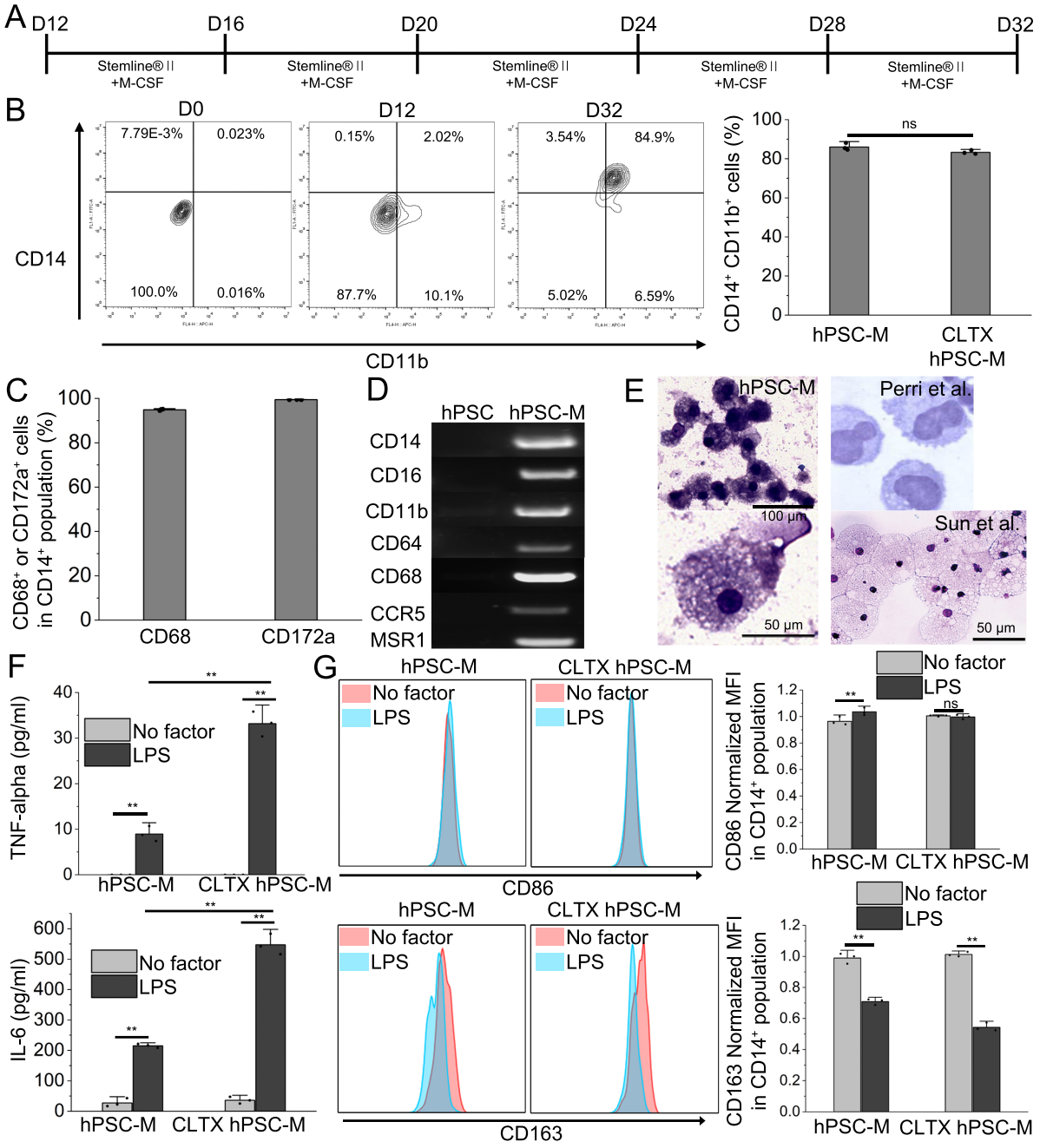


**Figure 3. Characterization of hPSC-derived macrophage-like cells (hPSC-M).** (A) Schematic of timeline for macrophage differentiation after day 12. Fresh Stemline II medium containing 50 ng/ml M-CSF is added every 4 days until day 32. (B) Flow cytometry analysis of CD14 and CD11b expression during and after macrophage differentiation. *n*=3 independent differentiations. (C) Flow cytometry analysis of CD68 and CD172a expression in $CD14^+$ hPSC-M. *n*=3 independent differentiations. (D) RT-PCR analysis of indicated macrophage makers on undifferentiated hPSC and hPSC-M. (E) Wright-Giemsa staining of hPSC-M. Staining images of macrophages from other studies [18,21] are included as controls. (F) Cytokine secretion from hPSC-M and CLTX hPSC-M with or without LPS treatment for

24 hours. Concentration of TNF-α and IL-6 in cell culture supernatant was measured by ELISA. The statistical analysis was performed using a one-way ANOVA with Tukey's host hoc test ($n$ = 3) (* $p < 0.05$ ** $p < 0.01$). (G) Flow cytometry analysis of CD86 and CD163 expression in $CD14^+$ hPSC-M and CLTX hPSC-M with or without LPS treatment for 24 hours. The expression level of CD86 and CD163 was presented as normalized median fluorescence intensity (MFI) (normalized to the MFI of the untreated condition). The statistical analysis was performed using a two-tailed Student's $t$-test ($n$ = 3) (* $p < 0.05$ ** $p < 0.01$). Data represented as mean ± SD.

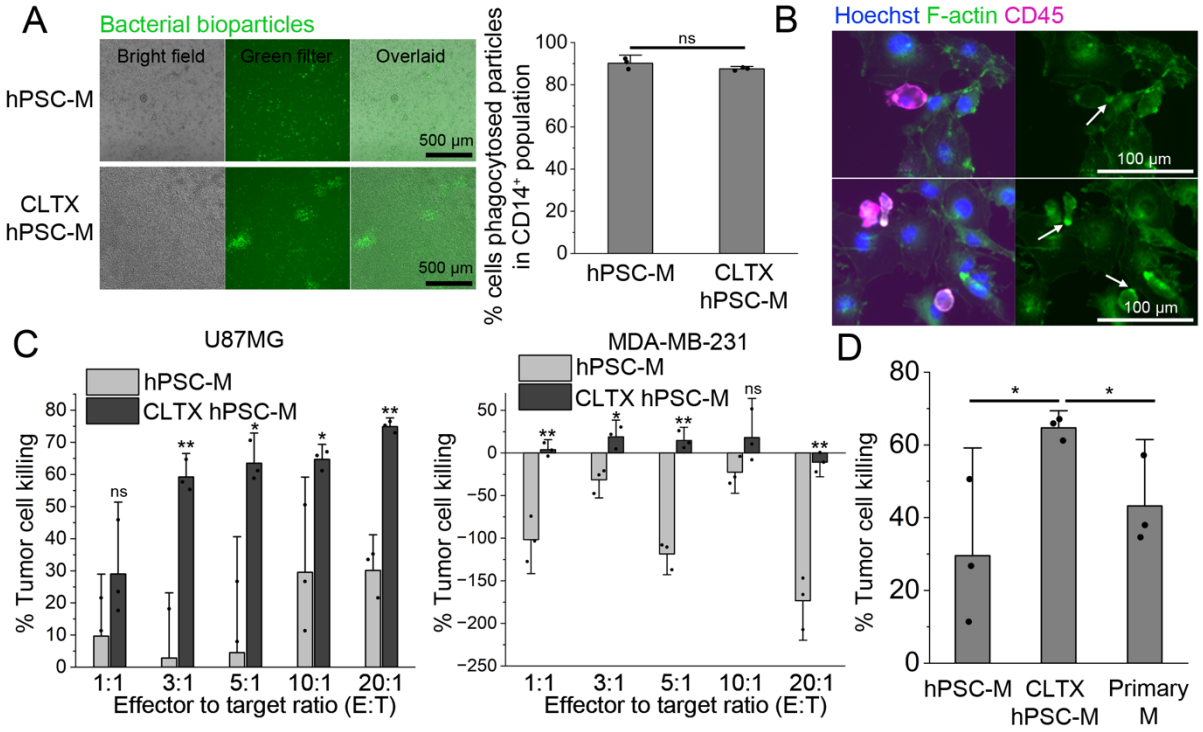


**Figure 4. Functional characterization of CLTX CAR hPSC-M.** (A) Phagocytosis assay using *E.coli* bioparticles. Unmodified hPSC-M and CLTX hPSC-M were incubated with the bioparticles for 12 hours and imaged under a fluorescence microscope. Brightfield images, images with green fluorescence filter, and overlaid images were shown. % cells phagocytosed particles among $CD14^+$ cells were measured by flow cytometry after CD14 staining. The statistical analysis was performed using a two-tailed Student's $t$-test ($n$ = 3) (* $p < 0.05$ ** $p < 0.01$). (B) Immunofluorescence images of CLTX hPSC-M for the expression of F-actin and CD45. The accumulation of F-actin (indicated with white arrow) was observed at the interface between $CD45^+$ CLTX hPSC-M (M) and U87MG tumor cells (Tu) as an evidence of immune synapse formation. (C) Cytotoxicity of unmodified hPSC-M and CLTX hPSC-M against luciferase-expressing U87MG and MDA-MB-231 cells. The effector and target cells were co-incubated for 24 hours and analyzed for luminous intensity. The % of tumor cell killing was calculated

by dividing the luminous intensity of the co-incubated well with that of the control (tumor cell only) well after background subtraction. The statistical analysis was performed using a two-tailed Student's *t*-test (hPSC-M *vs* CLTX hPSC-M) ($n = 3$) (* $p < 0.05$ ** $p < 0.01$). (D) Cytotoxicity of hPSC-M, CLTX hPSC-M and primary macrophages (Primary M) against luciferase-expressing U87MG at an effector-to-target cell ratio of 10:1. The statistical analysis was performed using a two-tailed Student's *t*-test (CLTX hPSC-M *vs* others) ($n = 3$) (* $p < 0.05$ ** $p < 0.01$). Data represented as mean ± SD.

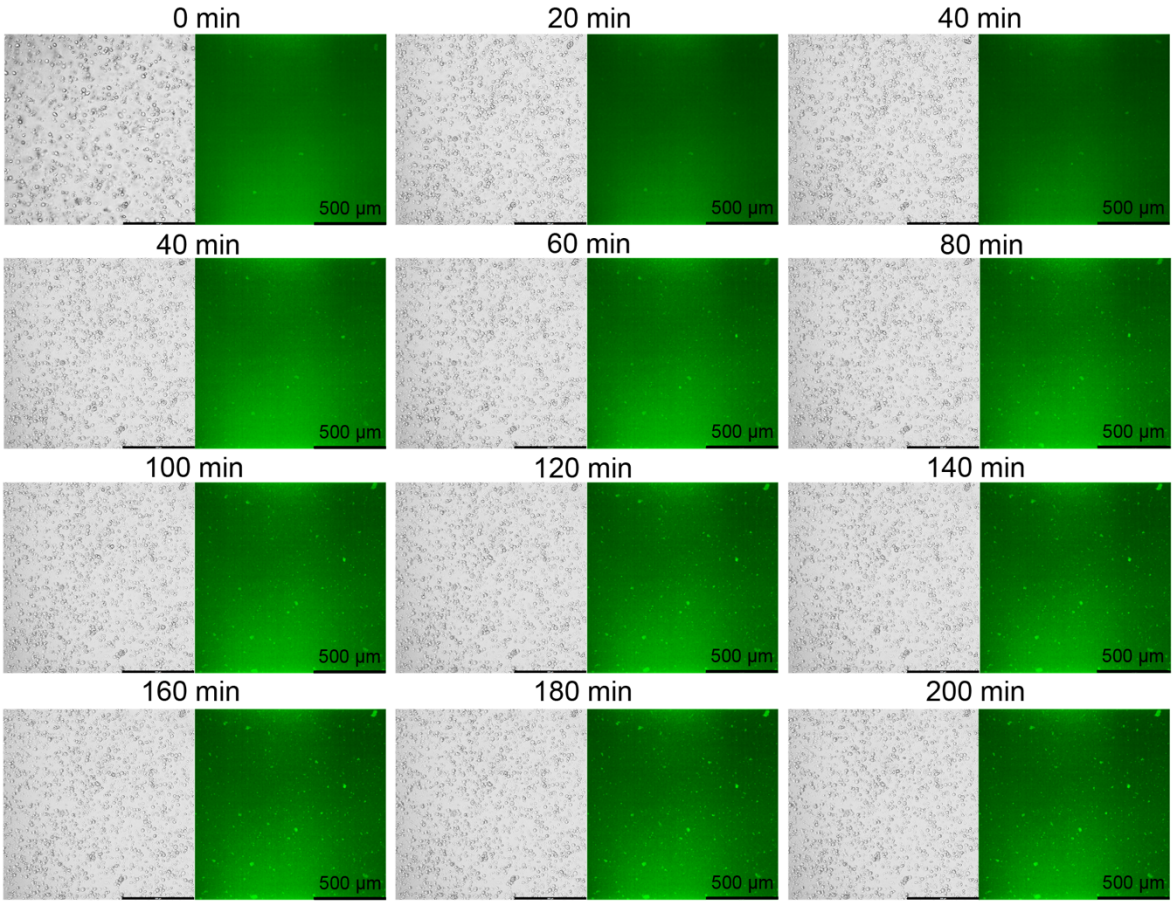


**Supplementary Figure 1.** Live cell images of hPSC-M after incubation with bacterial bioparticles. Images were captured at 20-minute intervals during the phagocytosis assay.

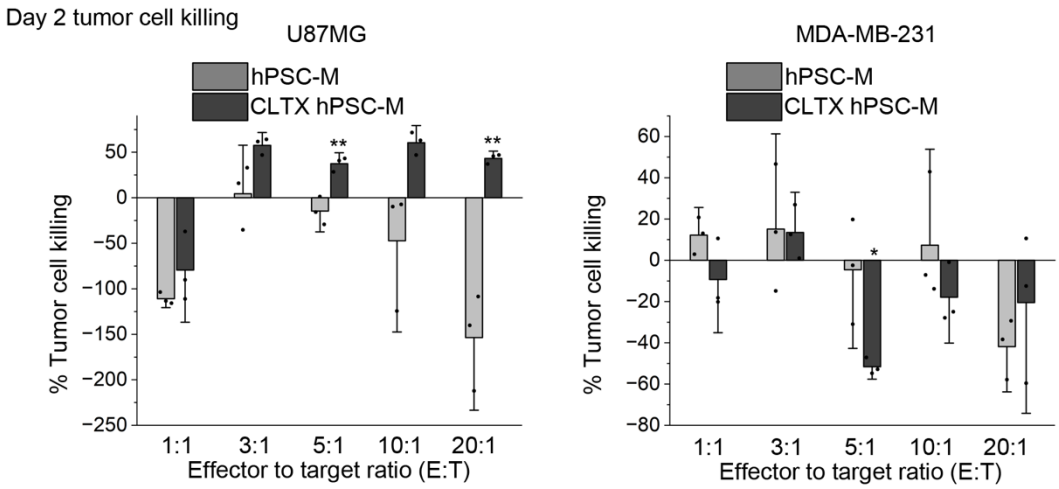


**Supplementary Figure 2.** Cytotoxicity of hPSC-M and CLTX hPSC-M against luciferase-expressing U87MG and MDA-MB-231 tumor cells after 48 hours of coculture. The statistical analysis was performed using a two-tailed Student's *t*-test (hPSC-M vs CLTX hPSC-M) ($n = 3$) (* $p < 0.05$ ** $p < 0.01$).

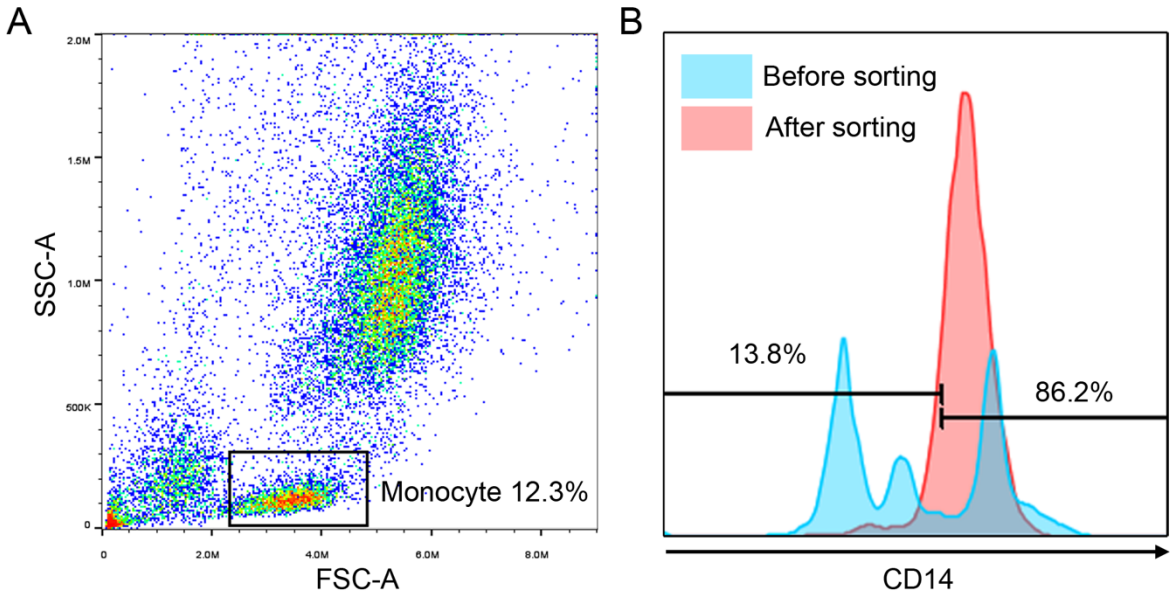


**Supplementary Figure 3. Isolation of primary monocytes.** (A) Flow cytometry analysis of a blood sample. Forward and side scatter plots demonstrate the typical separation of immune cells. (B) Isolation of $CD14^+$ monocytes by MACS analyzed by flow cytometry before and after sorting.


## Acknowledgements

We thank members of the Bao laboratory for technical assistance and critical reading of the manuscript. This study was supported by startup funding from the Davidson School of Chemical Engineering and the College of Engineering at Purdue (X.B.), NIH New R01

Program from Purdue University Office of Research (X.B.), and NIH NCI (grant no. R37CA265926 to X.B.). The authors also gratefully acknowledge support from the Purdue University Institute for Cancer Research, P30CA023168, Purdue Institute for Integrative Neuroscience (PIIN) and Bindley Biosciences Center, Purdue Institute for Drug Discovery Seed Award, National Science Foundation CAREER Award (grant no. 2143064 to X.B.), and the Walther Cancer Foundation.

**References**

1. McCune JS. Rapid advances in immunotherapy to treat cancer. *Clin Pharmacol Ther.* 2018; 103 (4): 540-544. https://doi.org/10.1002/cpt.985

2. CAR T Cells: Engineering Patients' Immune Cells to Treat Their Cancers. *National Cancer Institute* 2022. Accessed 31 Jan 2023. https://www.cancer.gov/aboutcancer/treatment/research/car-t-cells

3. Li YR, Dunn ZS, Zhou Y, Lee D, Yang L. Development of stem cell-derived immune cells for off-the-Shelf cancer immunotherapies. *Cells*. 2021;10(12):3497. https://doi.org/10.3390/cells10123497

4. Iriguchi S, Yasui Y, Kawai Y, Arima S, Kunitomo M, Sato T, Ueda T, Minagawa A, Mishima Y, Yanagawa N, Baba Y, Miyake Y, Nakayama K, Takiguchi M, Shinohara T, Nakatsura T, Yasukawa M, Kassai Y, Hayashi A, Kaneko S. A clinically applicable and scalable method to regenerate T-cells from iPSCs for off-the-shelf T-cell immunotherapy. *Nat Commun*. 2021;12(1):1-15.

5. Li Y, Hermanson DL, Moriarity BS, Kaufman DS. Human iPSC-derived natural killer cells engineered with chimeric antigen receptors enhance anti-tumor activity. *Cell Stem Cell*. 2018;23(2):181-192. e5. https://doi.org/10.1038/s41467-020-20658-3

6. Zhang L, Tian L, Dai X, Yu H, Wang J, Lei A, Zhao W, Zhu Y, Sun Z, Zhang H, Church GM, Huang H, Weng Q, Zhang J. Pluripotent stem cell-derived CAR-macrophage cells with antigen-dependent anti-cancer cell functions. *J Hematol Oncol*. 2020;13(1):1-5. https://doi.org/10.1186/s13045-020-00983-2

7. Jin G, Chang Y, Harris JD, Bao X. Adoptive Immunotherapy: A Human Pluripotent Stem Cell Perspective. *Cells Tissues Organs*. Published online 2023:1.

https://doi.org/10.1159/000528838

8. Chang Y, Syahirah R, Wang X, Jin G, Torregrosa-Allen S, Elzey BD, Hummel SN, Wang T, Li C, Lian X, Deng Q, Broxmeyer HE, Bao X. Engineering chimeric antigen receptor neutrophils from human pluripotent stem cells for targeted cancer immunotherapy. *Cell Rep*. 2022;40(3):111128. https://doi.org/10.1016/j.celrep.2022.111128

9. Wang D, Starr R, Chang WC, Aguilar B, Alizadeh D, Wright SL, Yang X, Brito A, Sarkissian A, Ostberg JR, Li L, Shi Y, Gutova M, Aboody K, Badie B, Forman SJ, Barish ME, Brown CE. Chlorotoxin-directed CAR T cells for specific and effective targeting of glioblastoma. *Sci Transl Med*. 2020;12(533):eaaw2672. https://doi.org/10.1126/scitranslmed.aaw2672

10. Chen Z, Feng X, Herting CJ, Garcia VA, Nie K, Pong WW, Rasmussen R, Dwivedi B, Seby S, Wolf SA, Gutmann DH, Hambardzumyan D. Cellular and molecular identity of tumor-associated macrophages in glioblastoma. *Cancer Res*. 2017;77(9):2266-2278. https://doi.org/10.1158/0008-5472.CAN-16-2310

11. Pan K, Farrukh H, Chittepu VCSR, Xu H, Pan C xian, Zhu Z. CAR race to cancer immunotherapy: from CAR T, CAR NK to CAR macrophage therapy. *J Exp Clin Cancer Res*. 2022. 2022;41(1):1-21. https://doi.org/10.1126/scitranslmed.aaw2672

12. Morrissey MA, Williamson AP, Steinbach AM, Roberts EW, Kern N, Headley MB, Vale RD. Chimeric antigen receptors that trigger phagocytosis. *Elife*. 2018; 7: e36688. https://doi.org/10.7554/eLife.36688

13. Zhang W, Liu L, Su H, Liu Q, Shen J, Dai H, Zheng W, Lu Y, Zhang W, Bei Y, Shen P. Chimeric antigen receptor macrophage therapy for breast tumours mediated by targeting the tumour extracellular matrix. *Br J Cancer*. 2019; 121 (10): 837-845. https://doi.org/10.1038/s41416-019-0578-3

14. Niu Z, Chen G, Chang W, Sun P, Luo Z, Zhang H, Zhi L, Guo C, Chen H, Yin M, Zhu W. Chimeric antigen receptor- modified macrophages trigger systemic anti- tumour immunity. *J Pathol*. 2021; 253 (3): 247-257. https://doi.org/10.1002/path.5585

15. Klichinsky M, Ruella M, Shestova O, Lu XM, Best A, Zeeman M, Schmierer M, Gabrusiewicz K, Anderson NR, Petty NE, Cummins KD, Shen F, Shan X, Veliz K, Blouch K, Yashiro-Ohtani Y, Kenderian SS, Kim MY, O'Connor RS, Wallace SR,

Kozlowski MS, Marchione DM, Shestov M, Garcia BA, June CH, Gill S. Human chimeric antigen receptor macrophages for cancer immunotherapy. *Nat Biotechnol*. 2020; 38 (8): 947-953. https://doi.org/10.1038/s41587-020-0462-y

16. Chang Y, Syahirah R, Oprescu SN, Wang X, Jung J, Cooper SH, Torregrosa-Allen S, Elzey BD, Hsu AY, Randolph LN, Sun Y, Kuang S, Broxmeyer HE, Deng Q, Lian X, Bao X. Chemically-defined generation of human hemogenic endothelium and definitive hematopoietic progenitor cells. *Biomaterials*. 2022;285:121569. https://doi.org/10.1016/j.biomaterials.2022.121569

17. Cao X, Yakala GK, van den Hil FE, Cochrane A, Mummery CL, Orlova VV. Differentiation and functional comparison of monocytes and macrophages from hiPSCs with peripheral blood derivatives. *Stem Cell Rep*. 2019; 12 (6): 1282-1297. https://doi.org/10.1016/j.stemcr.2019.05.003

18. Sun S, See M, Nim HT, Strumila K, Ng ES, Hidalgo A, Ramialison M, Sutton P, Elefanty AG, Sarkar S, Stanley EG. Human pluripotent stem cell-derived macrophages host Mycobacterium abscessus infection. *Stem Cell Rep*. 2022;17(9):2156-2166. https://doi.org/10.1016/j.stemcr.2022.07.013

19. Jo HY, Seo HH, Gil D, Park Y, Han HJ, Han HW, Thimmulappa RK, Kim SC, Kim JH. Single-Cell RNA sequencing of human pluripotent stem cell-derived macrophages for quality control of the cell therapy product. *Front Genet*. 2022;12:658862. https://doi.org/10.3389/fgene.2021.658862

20. Zhang J, Webster S, Duffin B, Bernstein MN, Steill J, Swanson S, Forsberg MH, Bolin J, Brown ME, Majumder A, Capitini CM, Stewart R,Thomson JA, Slukvin II. Generation of anti-GD2 CAR macrophages from human pluripotent stem cells for cancer immunotherapies. *Stem Cell Rep*. 2023;18(2):585-596. https://doi.org/10.1016/j.stemcr.2022.12.012

21. Perri SR, Annabi B, Galipeau J. Angiostatin inhibits monocyte/macrophage migration via disruption of actin cytoskeleton. *FASEB J*. 2007; 21 (14): 3928-3936. https://doi.org/10.1096/fj.07-8158com

22. Hirsch JG, Fedorko ME, Cohn ZA. Vesicle fusion and formation at the surface of pinocytic vacuoles in macrophages. *J Cell Biol*. 1968; 38 (3): 629.

https://doi.org/10.1083/jcb.38.3.629 26

23. Meng F, Lowell CA. Lipopolysaccharide (LPS)-induced macrophage activation and signal transduction in the absence of Src-family kinases Hck, Fgr, and Lyn. *J Exp Med*. 1997;185(9):1661-1670. https://doi.org/10.1084/jem.185.9.1661

24. Italiani P, Boraschi D. From monocytes to M1/M2 macrophages: phenotypical vs. functional differentiation. *Front Immunol*. 2014; 5: 514. https://doi.org/10.3389/fimmu.2014.00514

25. Davenport A, Cross R, Watson K, Liao Y, Shi W, Prince H, Beavis P, Trapani J, Kershaw M, Ritchie D, Darcy PK, Neeson PJ, Jenkins MR. Chimeric antigen receptor T cells form nonclassical and potent immune synapses driving rapid cytotoxicity. *Proc Natl Acad Sci*. 2018; 115 (9): E2068-E2076.

26. Mukherjee M, Mace EM, Carisey AF, Ahmed N, Orange JS. Quantitative imaging approaches to study the CAR immunological synapse. *Mol Ther*. 2017; 25 (8): 1757-1768.

27. Boutilier AJ, Elsawa SF. Macrophage polarization states in the tumor microenvironment. *Int J Mol Sci*. 2021; 22 (13): 6995. https://doi.org/10.3390/ijms22136995

28. Geribaldi-Doldán N, Fernández-Ponce C, Quiroz RN, Sánchez-Gomar I, Escorcia LG, Velásquez EP, Quiroz EN. The role of microglia in glioblastoma. *Front Oncol*. 2021; 10: 603495. https://doi.org/10.3389/fonc.2020.603495